Neurochemistry International 131 (2019) 104582

Contents lists available at ScienceDirect

Neurochemistry International

journal homepage: www.elsevier.com/locate/neuint

PKCε-dependent H-Ras activation encompasses the recruitment of the RasGEF SOS1 and of the RasGAP neurofibromin in the lipid rafts of embryonic neurons

Sophia Karouzaki, Charoula Peta, Emmanouella Tsirimonaki, Dimitra Mangoura*

Basic Research Center, Biomedical Research Foundation of the Academy of Athens, 4 Soranou Efesiou, Athens, 11527, Greece

ARTICLE INFO

Keywords:
Cannabinoids
Lipid rafts
PKCε
Neurofibromin
Neurofibromatosis
Ras

ABSTRACT

The spatial organization of plasma membrane proteins is a key factor in the generation of distinct signal outputs, especially for PKC/Ras/ERK signalling. Regulation of activation of the membrane-bound Ras, critical for neuronal differentiation and highly specialized functions, is controlled by exchanges in nucleotides catalyzed by nucleotide exchange factors (GEFs) for GTP loading and Ras activation, and by Ras GTPase Activated Proteins (RasGAPs) that lead to activation of the intrinsic GTPase activity of Ras and thus its inactivation. PKCs are potent Ras activators yet the mechanistic details of these interactions, or the involvement of specific PKC isoforms are now beginning to be addressed. Even less known is the topology where RasGAPs terminate Ras activation. Towards this aim, we isolated lipid rafts from chick embryo neural tissue and primary neuronal cultures when PKCε is the prominent isoform and in combination with in vitro kinase assays, we now show that, in response the PKCε-specific activating peptide ψεRACK, an activated PKCε is recruited to lipid rafts; similar mobility was established when PKCε was physiologically activated with the Cannabinoid receptor 1 (CB1) agonist methanandamide. Activation of H-Ras for both agents was then established for the first time using in vivo RasGAP activity assays, which showed similar temporal profiles of activation and lateral mobility. Moreover, we found that the GEF SOS1, and the major neuronal RasGAP neurofibromin, a specific PKCε substrate, were both transiently significantly enriched in the rafts. Finally, our in silico analysis revealed a highly probable, conserved palmitoylation site adjacent to a CARC motif on neurofibromin, both of which are included only in the RasGAP related domain type I (GRDI) with the known high H-RasGAP activity. Taken together, these results suggest that PKCε activation regulates the spatial plasma membrane enrichments of both SOS1 and neurofibromin, thus controlling the output of activated H-Ras available for downstream signalling in neurons.

1. Introduction

Posttranslational phosphorylations form the basis of membrane receptor signalling cascades and networks, as the imposed conformational changes on proteins drastically regulate their abilities to physically interact with membrane lipids and/or other proteins and thus propagate the signal laterally and inwards. The importance of phosphorylation relays during activation of the PKC/Ras/Raf/MEK/ERK1/2 pathway by membrane receptor in brain development and function has been well studied and documented (Bluthgen et al., 2017; Samuels et al., 2008; Zhu et al., 2001; Zisopoulou et al., 2013). Consistently, human mutations of ERK regulators cause an array of developmental disorders, such as Neurofibromatosis Type (NF-1) (Hyman et al., 2005), Costello (Aoki et al., 2005), and Noonan (Tartaglia et al., 2001) syndromes, all characterized potentially by learning disabilities or even mental retardation.

Protein Kinase C (PKC), a family of isoenzymes, exert their signalling role by specific phosphorylation of their substrate proteins, many of which are membrane-associated through lipid modifications. In their mature form, conventional (α, βI, βII, γ) and novel (δ, ε, θ, η, and μ)

Abbreviations: CB1, cannabinoid 1 receptor; CNS, central nervous system; ERK1/2, extracellular signal-regulated kinases 1/2; FGFR, fibroblast growth factor receptor; GAPs, GTPase-activating proteins; GEF, guanine nucleotide exchange factor; Gi, Gi protein; GPCR, G-protein-coupled receptor; Grb2, growth-factor-receptor binding protein 2; GRD, RasGAP related domain; GST, Glutathione S-transferase; Gq, Gq protein; MARCKS, myristoylated alanine-rich C-kinase substrate; MCD, methyl-beta-cyclodextrin; PKCε, protein kinase C epsilon; R(+)-MA, methanandamide; PLC, phospholipase C; PSD-95, postsynaptic density protein 95; RACKs, receptors for activated C-kinase; RBD, Ras-binding domain of Raf; RMA, R(+)-methanandamide; RTK, receptor tyrosine kinase; SOS1, Son of sevenless 1

* Corresponding author.
E-mail address: mangoura@bioacademy.gr (D. Mangoura).

https://doi.org/10.1016/j.neuint.2019.104582
Received 11 June 2019; Received in revised form 27 September 2019; Accepted 15 October 2019
Available online 17 October 2019
0197-0186/

PKCs stereospecifically bind to diacylglycerol (DAG), via their C1 zinc finger domains, which are thought to stabilize the active, deeply membrane-embedded state of PKCs (Zhang et al., 1995). Other PKC binding non-substrate proteins like the receptors for activated C-kinase (RACKs) may enhance their activity (Brandman et al., 2007). Uniquely among PKCs, PKCε is palmitoylated at least on cysteines 276 and 474 (Dasgupta et al., 2011) and the interplay of PKCε phosphorylation and lipidation mediates its plasma membrane targeting, while in turn, PKCε phosphorylation regulates the intracellular trafficking of its lipidated protein substrates (Gauthier-Kemper et al., 2014; Thelen et al., 1991), several of which play critical roles in dendritic spine plasticity and memory, e.g., the myristoylated alanine-rich C-kinase substrate (MARCKS) (Calabrese and Halpain, 2005; Mangoura and Dawson, 1993) or PSD-95 (Sen et al., 2016).

PKC activation has also documented roles in the activation of the small molecular weight GTPase Ras at the plasma membranes and in the formation of Ras and activated Raf-1 (MAPKKK) complexes (Mangoura et al., 2006; Marais et al., 1998; Zisopoulou et al., 2013) and thus the obligatory activation of the immediate kinases MEK (MAPKK) and ERK (MAPK) (Raman et al., 2007). Direct targets of PKC signalling for Ras activation may include Ras activators that belong to the GRP and SOS-families of GEFs (Ebinu et al., 1998; Kawakami et al., 2003; Leondaritis et al., 2009), even when PKC activation emanates from stimulation of GPCRs (O'Hayre et al., 2017). Indeed, the ongoing elucidation of the mechanistics of Ras activation by GPCRs appears to engage effectors that elicit Ras activation by activated receptor tyrosine kinases (RTKs), when a ligand-bound RTK and its docking proteins will recruit a GEF (guanine nucleotide exchange factor), e.g. SOS1 via its associated Grb2 (Ong et al., 2000), and SOS1-Ras binding will stimulate the release of bound GDP from Ras in exchange for GTP and hence Ras activation (Pechlivanis and Kuhlmann, 2006). The intrinsic GTPase activity of Ras.GTP is next accelerated by GAPs (GTPase-activating proteins), causing Ras to return to its inactive GDP state. Mutations or posttranslational modifications of RasGAPs lead to deregulation of Ras activity cycles and may contribute to abnormal neuronal function or tumor formation even when cells contain wild-type Ras, as in the case of the tumor suppressor neurofibromin, a RasGAP, which is mutated or deleted in NF-1 (Bollag et al., 1996; Mellert et al., 2018). While mechanistic details of the SOS1 recruitment to the membranes has been thoroughly investigated, the mechanism of membrane translocation of the heterogeneous group of RasGAPs is largely unknown (reviewed in Grewal et al., 2011; Scheffzek and Shivalingaiah, 2019).

H-Ras dynamically compartmentalizes in lipid rafts, the lipid-driven, relatively ordered fluid microdomains of the plasma membrane (e.g., Prior et al., 2001). Lipid rafts constitute nanoscale membrane assemblies, enriched in lipids, like cholesterol, glycolipids, and sphingolipids -albeit with different inner and outer membrane leaflet composition- and in GPI–anchored proteins and transmembrane receptors (e.g., Mangoura et al., 2016 and refs therein). Lipid rafts are regulatory for intracellular signalling, as most signalling molecules preferentially segregate at the lipid raft-cytosol interphase. Moreover, the dynamic regulation of protein modifications in the lipid rafts is what bestows on the rafts their functionality. For example the reversible protein palmitoylation may impart such raft affinity to both transmembrane and peripheral proteins (Levental et al., 2010; Salaun et al., 2005), as to possibly facilitate binding to cholesterol for proteins that contain CRAC or CARC consensus motifs (Fantini and Barrantes, 2013). However, what regulates the affinity of “soluble proteins” to lipid rafts during signalling is still under intense investigation, further emphasizing the importance of this mechanism.

This question becomes important for most RasGAPs that must transiently attain physical contact with the Ras proteins, especially for the major RasGAP in CNS neurons neurofibromin, the product of the *NF1* gene. *NF1* mutations cause Neurofibromatosis 1, a progressive disease with prominent and diverse symptoms in the CNS, ranging from learning disabilities (Hyman et al., 2005) to development of benign tumors and cancer in astrocytes (Brems et al., 2009), somewhat reproduced in conditional ablations of the gene in mice (Brown et al., 2010; Zhu et al., 2001). Neurofibromin is a multidomain, mobile protein (Li et al., 2001; Koliou et al., 2016) and studies on its protein sequence have begun to elucidate its known intracellular mobility and to explain the currently partial correlation of disease phenotypes and mutation genotypes (Koczkowska et al., 2018). Such research has been mostly conducted by over expressions and genetic manipulation of specific domains (Luo et al., 2014; Mangoura et al., 2006; Starinsky-Elbaz et al., 2009), as the full length gene has not been cloned and *nf1* knock out-mice are embryonic lethal (Brannan et al., 1994). Moreover, this collective experimental evidence by us and others has postulated that neurofibromin's distinct domains interact among them to interface with multiple proteins and coordinate signalling events that are central at least to neuronal and astrocytic function, the two cell types that neurofibromin is highly expressed throughout life and where most NF-1 symptoms stem from. Among these domains, the RasGAP related domain, GRD, is the most pertinent for investigating neurofibromin targeting to lipid rafts for the additional reason that it is also the locus for alternative splicing events. Thus, exon 31 (former 23a) is tightly regulated in favor of skipping in CNS neurons, and the produced transcript GRDI, is a very potent RasGAP in the yeast (Andersen et al., 1993) or ex vivo (Leondaritis and Mangoura, 2010), while inclusion of this exon is favored in astrocytes (reviewed in (Barron and Lou, 2012)) with the produced transcript GRDII being a weaker RasGAP. This alternative transcription is conserved among vertebrates (Andersen et al., 1993; Baizer et al., 1993; Koliou et al., 2016; Nishi et al., 1991), as is the sequence of the additional 63 nucleotides/21 amino acids and the respective exon-intron boundaries, all predicting functional significance.

With this background, we undertook these studies to begin to understand the mechanistics of if and how this RasGAP may be recruited to the plasma membranes during signalling by Cannabinoid Receptor 1 (CB1R), a palmitoylated, prominent GPCR in the CNS (Fedonidis et al., 2014; Oddi et al., 2012), recruited to lipid rafts upon activation (Asimaki et al., 2011).

2. Materials and methods

2.1. Materials

The PKCε-selective activator peptide ψεRACK [PKCε amino acids 85–92, HDAPIGYD] (Brandman et al., 2007) and the PKCε-selective inhibitor peptide εV1-2 [PKCε (amino acid 14–21), EAVSLKPT] were synthesized and conjugated to a peptide derived from the TAT human immunodeficiency virus protein, TAT 47–57 (YGRKKRRQRRR) via disulfide bonds by Peptide 2.0 Inc (Chantilly, VA, USA). CB1 receptor agonist R(+)-Methanandamide ((R)-N-(2-Hydroxy-1-methylethyl)-5Z,8Z,11Z,14Z-eicosatetraenamide), a synthetic, high affinity, and metabolically stable anandamide analog, and AM251 (N-(Piperidin-1-yl)-5-(4-iodophenyl)-1-(2,4-dichlorophenyl)-4-methyl-1H-pyrazole-3-carboxamide), a selective CB1 receptor antagonist, were purchased from Tocris Cookson (Avonmouth, UK), Gö6976 (5,6,7,13-tetrahydro-13-methyl-5-oxo-12H-indolo[2,3-a]pyr rolo[3,4-c]carbazole-12 propanenitrile) was from Calbiochem (Nottingham, UK), methyl-beta-cyclodextrin (MβCD) from Sigma-Aldrich (Steinheim, Germany); culture media and supplements were from Gibco, BRL (Paisley, UK) and fetal bovine serum (FBS) from Biowest (Nuaille, France). The following primary antibodies were used against: neurofibromin sc-67 (C-terminus) and sc-68 (N-terminus region), phosphorylated MARCKS, flotillin-1, phospho-PKCε-Ser729, neuroligin, H-Ras (rat monoclonal), and calnexin (Santa Cruz Biotechnology, SCBT, Heidelberg, Germany); H-Ras (clone Ras10) (Merck, Temecula, CA, USA); coatomer protein beta (β-COP) (Sigma, Steinheim, Germany); PKC-ε (ABCAM, Cambridge, UK); and Son of sevenless 1 (SOS1) (UBI, Lake Placid, NY). Species-specific antibodies conjugated to horseradish peroxidase or alkaline

phosphatase were from Jackson Immunoresearch (West Grove, PA, USA). S-hexylglutathione-agarose beads (GST-agarose) were from SCBT and Opti-Prep from Axis-Shield. All other standard reagents were purchased from Sigma or SCBT.

2.2. Methods

2.2.1. Tissue and primary neuron preparations

Telencephali (TL) were dissected from chick embryos on indicated embryonic days, were sliced and placed in 1 mL ice cold artificial cerebrospinal fluid (aCSF) (124 mM NaCl, 5 mM KCl, 1.25 mM NaH2PO4, 26 mM NaHCO3, 2 mM CaCl2, 1 mM MgCl2, and 10 mM dextrose) alone or with appropriate agents, agonists or antagonists. Pure cortical neuron cultures were prepared as previously described by us (e.g., (Asimaki et al., 2011; Asimaki and Mangoura, 2011; Cheng et al., 2000; Li et al., 2001). In short, telencephali from 8-day old chick embryos were dissected out of the diencephalon and the meninges using fine forceps under sterile conditions and dissociated mechanically using a nylon mesh of 48 μm. Neurons were plated on 100 mm poly-L-lysine-coated dishes (ratio 1 embryo/dish) in Dulbecco's modified Eagle medium (DMEM), containing 1% FBS and N2 supplement. Cultures were maintained at 37 °C and 7.5% CO_2/air. Under these conditions neurons attach and fully differentiate to synaptically coupled neurons, recapitulating the in ovo differentiation program (Cheng et al., 2000; Li et al., 2001; Mangoura et al., 1993). Treatments on primary neurons were done routinely after 3 or 4 days in culture. In several series of pilot experiments, profiles of proteins in membrane preparations at basal conditions or following treatments were almost identical in E9-13 telencephali and in E8-derived cultures at 4–7 days in culture.

2.2.2. Cell lysis and lipid rafts-membrane fractionations

For isolation of lipid rafts, we used a detergent-free fractionation protocol, which provides increased resolution of genuine-lipid rafts from caveolin-rich domains, non-raft plasma membranes, and intracellular ER and Golgi membranes (Macdonald and Pike, 2005), as shown for CB1R and FGFR in neurons (Asimaki et al., 2011; Mangoura et al., 2016). The enrichment of the first five fractions, considered as lipid rafts (Macdonald and Pike, 2005), in sphingomyelin, phosphatidylcholine, and cholesterol has been also verified for neural cells (Mangoura et al., 2016). In brief, 4–5 telencephali or 5 × 100mm neuronal cultures were resuspended in base buffer, consisting of 20 mM Tris-HCl pH 7.8, 250 mM sucrose, 1 mM $CaCl_2$, 1 mM $MgCl_2$, and protease and phosphatase inhibitors, and then lysed by repeated passage through a 23G needle. Lysates were centrifuged at 1000 × *g* for 10 min and 4 × 25 μL of the resulting postnuclear supernatant were assessed for protein content using the Biorad DC kit, after the addition of Triton X-100 to a final concentration of 0.1%. Five mg of protein per condition were then mixed 1:1 with 50% OptiPrep, and an 8 ml 0–20% OptiPrep gradient in base buffer was carefully laid on top; gradients were centrifuged for 90 min at 52,000 × *g* using a TH-641 rotor in a Sorval ultracentrifuge and 14 × 700 μL continuous fractions were collected; 100 μL were precipitated with trichloroacetic acid for protein content estimation and the rest of each fraction was boiled in Laemmli buffer. Typically, protein content almost doubled per group of membrane fractions, and therefore it was essential to normalize each Western blot densitometry value per total protein of the corresponding fraction (e.g., Fig. 1).

2.2.3. Renaturation and assay of protein kinases

Detection of PKCs and other serine/threonine kinases that phosphorylate myelin basic protein (MBP) in vitro was performed as previously described (Mangoura and Dawson, 1998). In brief, equal amounts of protein from pooled lipid rafts fractions (1–5) were resolved by SDS- electrophoresis in 8% polyacrylamide gels containing 0.1 mg/mL MBP. Gels were then incubated in a HEPES – buffer to allow renaturation of proteins and kinases and subsequently incubated in the

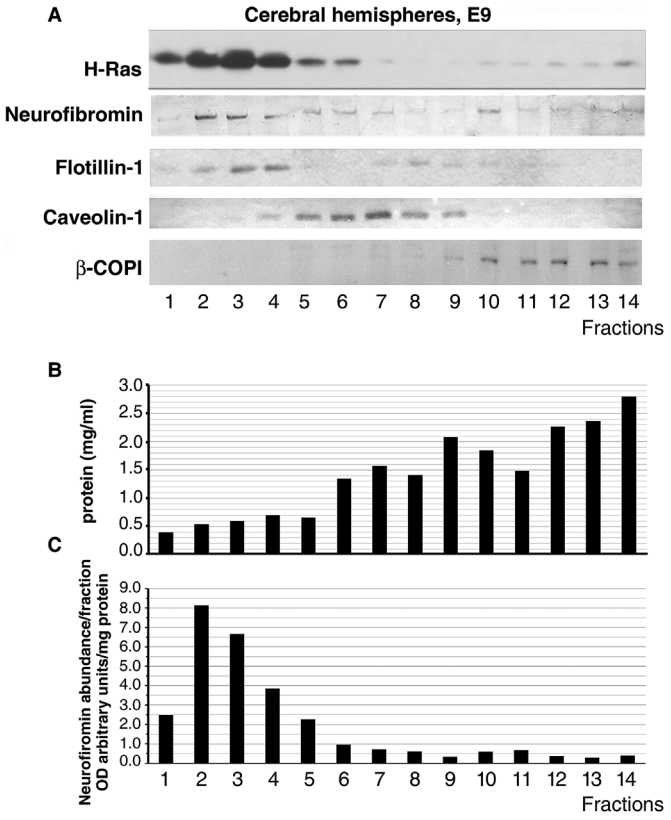

Fig. 1. Membrane distribution of neurofibromin in embryonic neurons. **A.** Frames contain representative images from detergent-free membrane preparations of neurons dissociated from 9-day-old chick embryo telencephalon, analyzed by SDS-PAGE (each lane contains a 50 μl aliquot from each of the 14 OptiPrep gradient fractions) and Western blotting with indicated antibodies. **B.** Characteristic protein content distribution of detergent free lipid raft fractionation, showing significantly less protein content in the lipid raft fractions; bars represent means from 4 experimental series (SEM ≤ 5% in all cases). **C.** Densitometry analysis of Western blot scans from these series and subsequent normalization of the measurements means over protein content per fraction reveals the extend of neurofibromin enrichment in neuronal lipid rafts.

presence of [^{32}P] -ATP, Mn^{+2}, and Mg^{+2} (1 h, 30 °C), stained with Coomassie Brilliant Blue, dried, and processed for autoradiography. Bands on the autoradiograms signify the molecular weight of in vivo activated serine/threonine kinases, which phosphorylate MBP in vitro. Gel areas corresponding to 90-92kD were excised, quantitated by scintillation counting, and kinase activity was expressed as cpm of transferred [^{32}P] phosphate. In pilot experiments the excised bands were processed for Western blotting with specific anti- PKCε antibodies to verify the identity of the kinase.

2.2.4. Measurement of GTP-bound state of Ras

Activated Ras was assessed by affinity precipitation, as we have previously described (Leondaritis and Mangoura, 2010; Mangoura et al., 2006), from 1 mg of protein per condition, using as bait a fusion protein of GST and the Ras-binding domain of c-Raf (GST-c-Raf-1-RBD), which specifically recognizes activated Ras (de Rooij and Bos, 1997). In short, neuronal lysates (in 50 mM Tris pH 7.5, $MgCl_2$ 20 mM, NaCl 150 mM, 1% NP-40, and 10% glycerol, containing a protease inhibitor cocktail (Sigma), 2 mM NaF, 1 mM sodium orthovanadate, 1 mM sodium molybdate, and 100 μg/mL PMSF) clarified by centrifugation were incubated (1 h at 4 °C) with freshly prepared GST-c-Raf-RBD, conjugated to glutathione-agarose beads. The GST-RBD-agarose beads were washed extensively, and the amounts of activated Ras precipitated by GST-RBD were determined by Western analysis, in parallel with 30 μg of total neuronal lysates for additional normalization (Fig. 3).

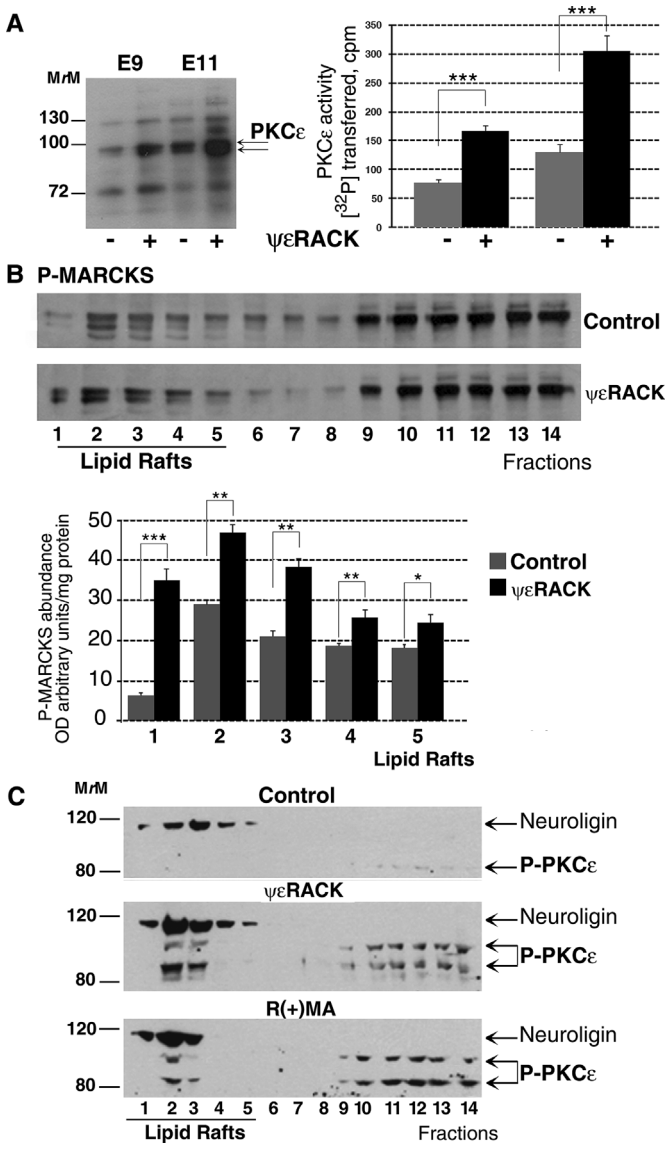

Fig. 2. Activated PKCε is highly detected in pooled lipid rafts of Differentiated Neurons. A. Highly pure, detergent free lipid rafts (fractions 1–5, 2.2.2), prepared from E9 and E11 chick embryo telencephali treated with vehicle or with [1 μM] ψεRACK for 5 min, were pooled and renatured kinases were assayed (2.2.3) for phosphorylation of MBP; frame contains a representative autoradiography example. In all experiments, gel areas corresponding to signals at 90–92 kDa were excised and [^{32}P] incorporation was quantitated by scintillation counting; bracketed bars in graph represent the means ± SEM from three experiments. **B.** Sister membrane preparations (E11), analyzed for phosphorylated MARCKS (P-MARCKS) detection with Western blotting (lanes contain 50 μl aliquots from each OptiPrep gradient fraction, 2.2.2), show statistically significant enrichment (graph) of this PKC substrate to lipid rafts. Data (columns) in A and B are the mean values ± SEM values from four different experiments, *** significant at $P < 0.01$ ** at $P \geq 0.01$, and * at $0.05 > P > 0.02$. **C.** Sister membrane preparations (E11) were also analyzed by Western blotting for P-PKCε^{ser726} to show detection of this phosphorylated PKCε species only upon activation with ψεRACK or Methanandamide (R(+)-MA). Blots were subsequently blotted with an antibody to the integral membrane protein neuroligin to validate the preparations; experiments were repeated 3–4 times, yet statistics were not performed as P-PKCε^{ser726} in controls was below detection levels.

2.2.5. Western blot analysis

Analysis was essentially done as previously described (Asimaki et al., 2011; Asimaki and Mangoura, 2011; Cheng et al., 2000; Mangoura et al., 2006). Equal volumes (50 μl) of OptiPrep fractions in Laemmli buffer were loaded per well and separated with SDS-PAGE. After electrophoresis, proteins were transferred into nitrocellulose membranes and probed with primary antibodies; in some cases membranes were stripped and reprobed, unless established high specificity of antibodies against proteins with distinctly different M_r allowed sequential Western blotting (Asimaki et al., 2011; Asimaki and Mangoura, 2011; Cheng et al., 2000; Mangoura et al., 2006). Immunoreactivity was visualized by further incubation with the appropriate species-specific antibody conjugated to horseradish peroxidase (HRP) and ECL chemiluminescence. Typically, all conditions within experiments were developed on the same film sheet and same exposure times per epitope. Exposed films or stained membranes were then scanned and densitometry analysis was performed with the densitometry software ImageJ (Asimaki et al., 2011; Mangoura et al., 2006).

2.2.6. Statistical analysis

All experiments were performed three to ten times with similar results and numerical data were analyzed by ANOVA.

2.2.7. Databases

The following databases have been used: genome browser www.ensembl.org/index.html; sequence analysis: https://www.ebi.ac.uk/Tools/emboss/; and prediction of post translational modifications https://www.expasy.org/tools/#ptm.

3. Results

Aberrations in morphology and density of dendrites are evident in NF-1 patients (Hyman et al., 2005), as predicted by earlier developmental studies in model systems by others and us (Li et al., 2001; Lin et al., 2007; Oliveira and Yasuda, 2014). For the chick embryo neurofibromin expression peaks first at the onset of differentiation at E8, a developmental point by which most neurons have been generated and constitute the vast majority of the CNS cell population (Li et al., 2001; Mangoura et al., 1993), and then again with synaptogenesis (Li et al., 2001), processes that are under intense regulation of Ras activation (Alpar et al., 2008; Seeger et al., 2003). However, despite the demonstration that PKC-phosphorylation of neurofibromin is required for its function as a GAP for the membrane-bound Ras (Mangoura et al., 2006), whether and how the assumed but not previously shown recruitment of neurofibromin to membranes occurs in neurons or any other cell type, has not been addressed.

3.1. Neurofibromin and activated PKCε are highly enriched in the lipid rafts in developing neurons

To investigate the molecular events that contribute to the recruitment of neurofibromin to plasma membranes, we first examined neurofibromin localization in neuronal membranes, using 9- through 13-day-old chick embryo telencephali or E8 primary neurons and the subcellular fractionation method which allows considerable resolution of lipid rafts, caveolin-rich domains, non-raft plasma membranes, and intracellular ER and Golgi membranes (Asimaki et al., 2011; Macdonald and Pike, 2005). Thus, equal volumes (50 μL) from each fraction were loaded on appropriate percentage gels and the resulting Western blots (Fig. 1A) were quantitated by densitometry, after normalizing over total protein loaded per well (Fig. 1 B and C) in order to best appreciate enrichments (Asimaki et al., 2011). We found that indeed neurofibromin is enriched in the same fractions that both typical rafts resident proteins H-Ras and flotillin-1 are (Fig. 1A), or up to a 4-fold level over the rest fractions (Fig. 1C), less so in the caveolin-rich fractions, while some neurofibromin pools were also detected in Golgi membranes (as identified by β-COPI, 1A and C), especially in fraction 10.

As we have previously demonstrated that PKCε, a major PKC in differentiating neurons (Mangoura and Dawson, 1993; Mangoura et al., 1993), specifically phosphorylates neurofibromin to increase its

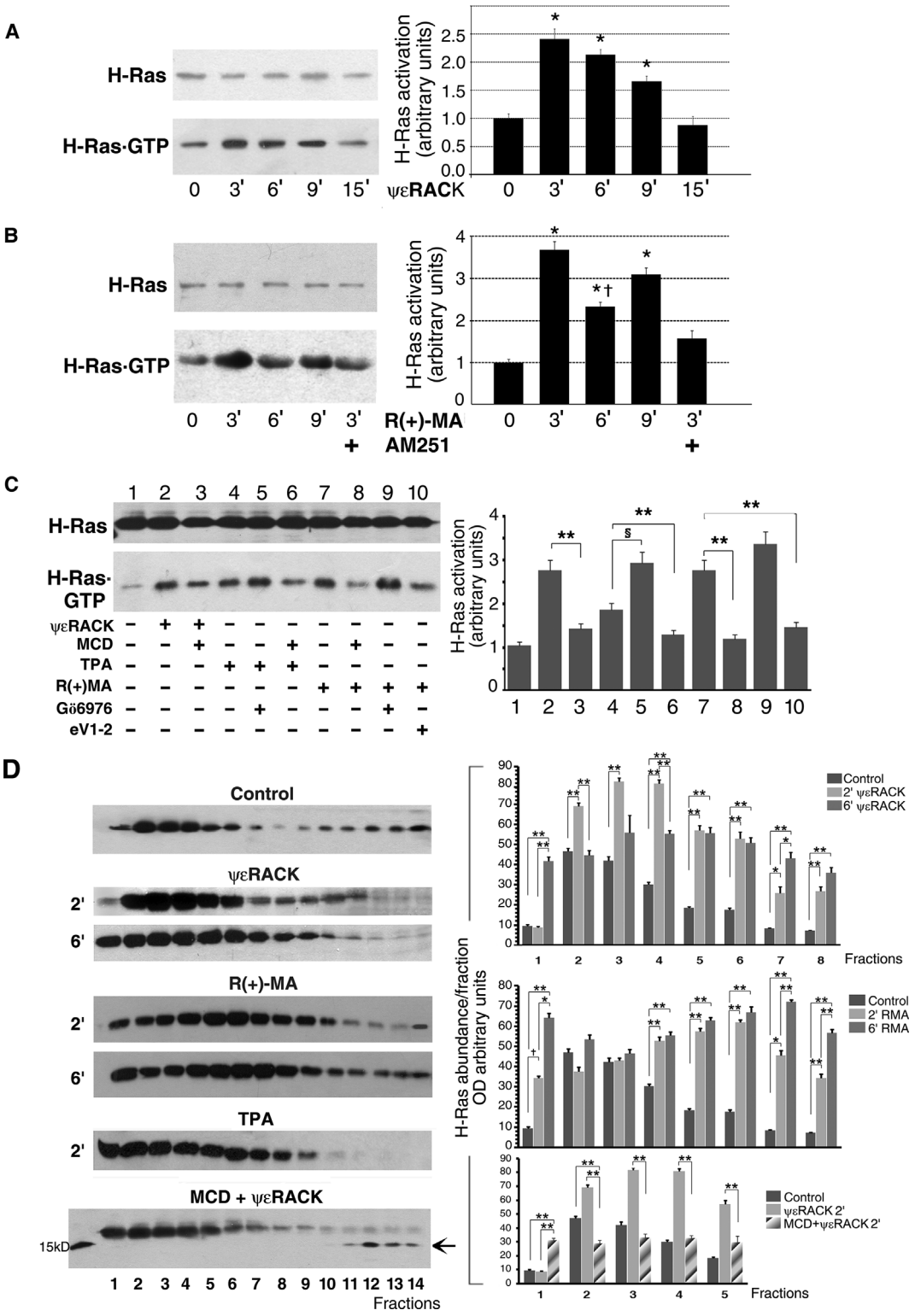

(caption on next page)

RasGAP activity (Mangoura et al., 2006), we sought to explore whether we may detect PKCε activity in raft fractions, where the highest neurofibromin enrichment was detected. Functional activation of PKCε was established using an MBP-kinase renaturation assay in pooled lipid raft fractions (1–5) from two embryonic days, E9 and E11 (Fig. 2), which express increasingly higher levels of PKCε (Mangoura et al., 1993). Thus, telencehali were acutely treated with vehicle or with ψεRACK, a selective peptide agonist of PKCε (2.1) and when equal samples of total cell homogenate from these preparations were separated in gels containing MBP and then reacted in vitro with [γ-^{32}P]ATP (2.2.3), seven renaturable MBP kinases were identified as activated in the lipid rafts (Fig. 2A). Western blot analysis of the excised bands of M_r of 90–92 verified what the molecular weight alone indicated, that is, strong activation of PKCε by 5 min of treatment with [1 μM] ψεRACK. At the same time frames, ψεRACK induced the recruitment of the PKC-specific substrate MARCKS, an actin-binding protein essential for several

Fig. 3. PKCε regulates H-Ras-GAP activity in embryonic neurons from E7 telencephali, 5 days in culture.
A. Direct activation of PKCε with ψεRACK [1 μM] elicits time-dependent activation of H-Ras in neuronal cultures. Frames contain the scans of typical Western blots with a rat monoclonal antibody against Ras from total neuronal lysate (upper frame, 30 μg protein/lane in a 15% SDS polyacrylamide gel) and of active Ras.GTP (lower frame) isolated with affinity precipitation from 500 μg of neuronal proteins, using GST-RBD as a bait. **B**. Methanandamide (R(+)-MA)-induced H-Ras activation is biphasic and is abolished by the specific CB1 antagonist AM251 [5 nM], applied 5 min prior to R(+)-MA. Frames contain the scans of typical Western blots as in A: upper frame depicts detection of H-Ras in total neuronal lysate and lower frame detection of active Ras.GTP. **C.** Sensitivity of H-Ras activation to cholesterol depletion and to specific inhibition of PKCε. Panel shows the effects on ψεRACK-, TPA-, or R(+)-MA-stimulated activation of H-Ras of a. cholesterol depletion with preincubation of cells with methyl-β-cyclodextrin (MCD) (10 mM × 2 min); b. classic PKCs inhibition with Gö6976 (1 μM × 10 min); and c. PKCε inhibition with the PKCε-selective inhibitor peptide eV1-2 (1 μM × 15 min) (H-Ras is detected with the mouse monoclonal antibody Ras 10). **D**. H-Ras activating agents ψεRACK, R(+)-MA, or TPA induce a time-dependent lateral mobility towards both the lowest density fractions and the less lipid-ordered fractions, an event abolished by pretreatment with partial cholesterol depletion (MCD); in the last frame right arrow denotes a lower than 21kD H-Ras reactive band and left the M_r marker of 15kD. All graphs contain densitometry analysis data after normalization of H-Ras.GTP densities over total H-Ras; data (columns) are the mean values ± SEM values from 4 to 5 different experiments, **P ≤ 0.01, *P < 0.02 over vehicle incubation, †P < 0.02 significance between 3 or 9 min against 6 min of R(+)-MA, §P < 0.02 TPA alone over pre-incubation with Gö6976, and + P ≤ 0.05.

important lipid raft dependent-functions, such as spine activity (Calabrese and Halpain, 2005; Yamaguchi et al., 2009), further establishing that PKCε-induced phosphorylation may direct its neuronal substrates to lipid rafts (Fig. 2B, panels and graph).

Opting to investigate in addition PKCε activation by a membrane receptor, we included in our analysis agonism of CB1R, a receptor that we have previously shown to rapidly incorporate into lipid raft fractions upon agonist binding, a prerequisite for CB1R proximal signalling (Asimaki et al., 2011), a cascade mediated by PKCε activation (Asimaki and Mangoura, 2011). As expected from previous studies with ψεRACK in rat hippocampi (Zisopoulou et al., 2013) and nucleus pulposus cells (Tsirimonaki et al., 2013) or Methanandamide (R(+)-MA) in chick embryonic neurons (Asimaki et al., 2011; Asimaki and Mangoura, 2011), both agents significantly increased phosphorylation of PKCε on Serine 729 (Fig. 2C), a necessary phosphorylation of activation. Moreover, the Ser729-phosphorylated species of PKCε were primarily detected in the lipid rafts and lesser in the endocytic membranes (9–12) only after exposure to ψεRACK or R(+)-MA. This lack of detection of P-PKCε in the controls led us to regularly re-blot the nitrocellulose membranes with an antibody to neuroligin, an integral membrane protein, as a control for proper cell membrane preparations (Fig. 2C). P-PKCε detection was diminished by preincubation with either the cholesterol sequestering agent methyl-β-cyclodextrin (MCD) or, in the case of R(+)-MA, also with the PKCε-selective inhibitor peptide εV1-2 (data not shown). Taken together, these data showed that an activated PKCε and its substrates are recruited to the rafts.

3.2. Direct or cannabinoid 1 receptor-dependent PKCε-activation leads to H-Ras activation

We next examined whether PKCε activation led to activation of Ras. Thus, primary neuronal cultures were acutely treated with either [1 μM] ψεRACK or [10 nM] Methanandamide (R(+)-MA), a stable anandamide analog, and equal amounts of neuronal lysate protein (Fig. 3A and B, upper frames) were processed for Ras.GTP affinity precipitation assays, which use the Ras-binding domain of Raf (GST-RBD immobilized on S-hexylglutathione-agarose beads) as a bait (A and B lower frames). As shown in Fig. 3, we found that both ψεRACK or R(+)-MA activated Ras in a time-dependent manner, albeit with different profiles. ψεRACK induced a maximal Ras activation within 3 min that slowly dissipated thereafter, returning to basal levels by 15 min (Fig. 3A). Exposure of neurons to R(+)-MA, however, elicited an activation profile with fluctuating levels (Fig. 3B, lower frame): by 3 min of R(+)-MA levels of activated Ras were 4-fold as compared to neurons treated with vehicle, levels were only twice as high after 6 min, and, levels rose again up to 3.5-fold by 9 min. As expected, this activation was suppressed after pretreatment of neurons with the potent and selective CB1R antagonist AM251, which at [5 μM] blocked the CB1R-mediated activation of Ras. The observed fluctuation most likely reflected a positive feedback loop, expected from the biphasic ERK activation that we have previously analyzed as stemming from transactivation of FGFR in neurons (Asimaki and Mangoura, 2011).

Furthermore, H-Ras activation by both ψεRACK or R(+)-MA as well as by the phorbol ester 12-O-tetradecanoyl-phorbol-13-acetate (TPA, 1 nM) was sensitive to membrane cholesterol depletion with methyl-β-cyclodextrin (MCD) (Fig. 3C, lanes 2, 4, and 7 versus 3, 6 and 8, respectively), at least to the extend of cholesterol removal (~50% with either 10 mM MCD for 2 min or 2 mM for 10 min). Interestingly, the staurosporine derivative Gö6976 that inhibits all Ca^{2+}-dependent, classic but not the novel PKC isoforms significantly enhanced H-Ras activation by TPA and R(+)-MA (lanes 5 and 9), possibly indicating a negative feedback regulation by the classic PKCs. Finally, the PKCε-selective inhibitor peptide eV1-2 significantly inhibited the R(+)-MA-induced H-Ras activation (Fig. 3C, lane 10), further establishing that the major effector of activate CB1 receptors is PKCε.

In our multiple independent experiments we also found that acute exposure to ψεRACK, R(+)-MA, or TPA altered the lateral mobility of H-Ras, however, this mobility could not be directly associated with the state of activation of Ras in these preparations, as the antibodies may not distinguish between GTP- or GDP-bound H-Ras. More specifically, we found that in all instances, there was a statistically significant enrichment of H-Ras in rafts, most notably in fractions 1, 4 and 5 (Fig. 3D panels and graphs), which continued even when H-Ras was prominently detected in the higher density fractions 6–8. Taken together with the affinity precipitation assays, this Western blotting analysis appeared to capture the movement of H-Ras out of the rafts upon its activation, a predicted event (Prior et al., 2001), and, with the same token, the enrichment in the rafts throughout these cycles of activation. As it is not possible to perform trustworthy experiments in this design with shorter than 2 min exposures, it is possible that we may have lost events that occur in a scale of seconds or less. Nevertheless, the same pattern of H-Ras distribution upon activation, that is enrichment in all raft fractions as well as in the less ordered fractions 6–8, was observed with TPA (Fig. 3D). The observed mobilities within neuronal membranes were not recorded when cells were preincubated with MCD, the only instance that an additional band of ~18kD was detected in the last fractions 9–14 (Fig. 3D, right arrow), feasibly denoting H-Ras degradation (Kim et al., 2009). These experiments collectively showed for the first time that direct PKCε activation leads to activation of H-Ras, as well as demonstrated CB1-dependent Ras activation, which has been implied (e.g., Asimaki and Mangoura, 2011), but not actually shown before.

3.3. The RasGEF SOS1 accumulates to lipid rafts in response to direct or cannabinoid 1 receptor-dependent activation of PKCε

Having established the peak time of Ras activation at 3 min, we next sought to establish whether PKCε activation leads to activation of Ras by inducing membrane recruitment of the RasGEF SOS1. As shown in Fig. 4, SOS1 is practically all cytosolic at basal conditions, while with activation of PKCε directly with ψεRACK or after R(+)-MA agonism it is recruited primarily to the highly ordered fractions 2 and 3, as early as 2 min. It must be noted that, within this short time of exposure, SOS1 is

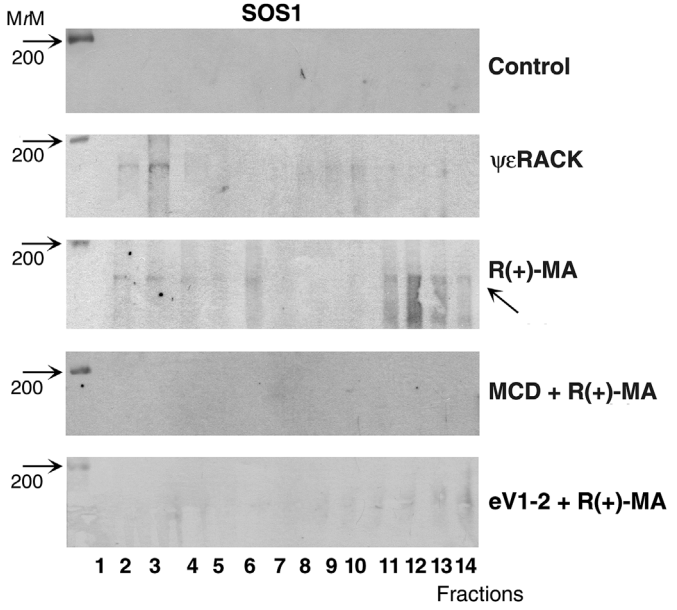

Fig. 4. SOS1 is recruited to lipid rafts upon PKCε activation.
Frames contain representative images from detergent-free membrane preparations of primary neurons from 8-day-old chick embryo telencephali exposed, at 5 days in culture, to vehicle, the PKCε activating peptide ψεRACK [1 μM], the selective CB1 agonist methanandamide (R(+)-MA), or to R(+)-MA after pretreatment with methyl-β-cyclodextrin (MCD) [10 mM] for 2 min or the selective PKCε inhbitory peptide eV1-2. Each lane contains a 50 μl aliquot from each OptiPrep gradient fraction, which was then analyzed by SDS- 8%-polyacrylamide gel electrophoresis and by Western blotting with specific antibodies (2.1); left arrows point to the 200kD pre-stained marker and right arrow points to increased SOS1 detection in Golgi membranes.

already detected in the endocytic membranes, which further emphasizes, along with the lack of detection in the lipid rafts in baseline conditions or any time after 3 min (not shown) and along with its ceasing with pretreatment of cells with the cholesterol sequestering agent methyl-β-cyclodextrin (MCD) or with the PKCε-selective inhibitor peptide eV1-2, that indeed SOS1 membrane trafficking to the rafts upon PKCε activation is specific, transient, and one-way (Christensen et al., 2016).

3.4. The RasGAP neurofibromin and its phosphorylating kinase PKCε accumulate to lipid rafts, upon direct (ψεRACK) or cannabinoid 1 receptor-dependent activation of PKCε

As regulation of an expected neurofibromin targeting to membranes has not been previously addressed or postulated, we sought to investigate whether its only demonstrated post-translational modification, that is phosphorylation by PKCε, may play a role. Thus sections of E11 chick telencephali were exposed to vehicle, the PKCε activating peptide ψεRACK, or methanandamide for 3 min and then all membrane fractions were studied by Western blotting and densitometry on the same nitrocellulose membrane for detection of neurofibromin and PKCε. Our analysis revealed that, upon treatment with ψεRACK, and therefore PKCε activation, neurofibromin abundance in the lipid rafts increased by 2,5-fold (Fig. 5A and graph B); almost as drastic was neurofibromin's lipid raft recruitment after activation of CB1R with R(+)-MA (Fig. 5A and graph B). Interestingly, while the association of neurofibromin with all membranes was higher in both cases than that with exposure to vehicle, the distribution appeared different with direct activation or with CB1R-signal dependent activation of PKCε. Thus, ψεRACK induced enrichment in the lipid raft and in the first caveolae fractions (1–5) whereas, following CB1-dependent signalling, neurofibromin was highly enriched only in fractions 2 and 3, as well as in the endocytic membranes (9–12). Differential increases and distribution were also observed for PKCε (Fig. 5A). While ψεRACK induced a 2-fold enrichment of PKCε in the rafts fractions (5D) primarily in fractions 2 and 3 (5E), R(+)-MA imposed a greater, 5-fold enrichment in the rafts (5D) that included high contributions by fraction 1 (5E). Taken together these results postulate for the first time that an activated PKCε and its phosphorylated substrate RasGAP neurofibromin are specifically recruited to lipid rafts.

4. Discussion

In this study, we show that direct or Cannabinoid receptor 1-driven activation of PKCε activates Ras and concomitantly induces the membrane recruitment of the RasGEF SOS1 to lipid rafts, as well as the suspected and now demonstrated targeting to membranes of the RasGAP neurofibromin.

Using lipid rafts preparations in combination with in vitro kinase renaturation assays, we now postulate that an activated, by its selective peptide activator ψεRACK, PKCε is highly enriched in neuronal lipid rafts, and, as a functional consequence, the PKC-specific substrate MARCKS was also detected phosphorylated there, even in the lowest density fraction 1 (Fig. 2). While these data resolve a conflict on PKCε translocation to the rafts, when rafts were isolated as detergent insoluble/resistant membrane domains (Cabrera-Poch et al., 2004; Lang et al., 2002), they also support the notion that, upon kinase-activating phosphorylations as after CB1 agonism (Asimaki and Mangoura, 2011, Fig. 2C), PKCε is also palmitoylated (Sanders et al., 2015) on cysteines 276 and 474 in a positive feedback manner (Dasgupta et al., 2011). Since most soluble signalling proteins require usually a second event for more stable membrane anchoring (Pechlivanis and Kuhlmann, 2006; Smotrys and Linder, 2004) and given the association of PKCε with cholesterol-rich domain that we now show (Figs. 2 and 5), we proceeded to analyze in silico cholesterol binding motifs on PKCε. This analysis revealed that human PKCε has seven cholesterol binding motifs of the CARC type [K/R)-X1-5-(Y/F)-X1-5-(L/V)] and gga PKCε has two more, with both species baring three of the CRAC type [(L/V)-X1-5-(Y)-X1-5-(K/R)] motifs. Notably, in both species and in the rat the experimentally verified palmitoylated Cys 276 (Dasgupta et al., 2011) is in close proximity with CARCS, while the other such site Cys 474 is in the middle of a sequential CARC-CRAC-CARC conserved motif of 21 amino acid (Scheme 1).

Taking analogy from the mono-palmitoylated β2-adrenergic receptor dimer, where one pair of cholesterol molecules packs within the hollow that forms between two palmitoyl residues (each offered by one β2-AR (Cherezov et al., 2007)), we may surmise that these predicted and verified lipid modification sites synergistically and in relation to kinase-activating phosphorylations regulate the recruitment of PKCε to lipid rafts.

Especially for PKCε activation with CB1 agonism, we should additionally consider that in basal conditions PKCε physically associates with CB1R, and that this interaction is resolved upon ligand binding, allowing PKCε to physically associate and activate tyrosine kinases Src and Fyn (Asimaki and Mangoura, 2011). It is thus feasible, that recruitment of an activated PKCε to the lipid rafts is facilitated by interactions first with CB1 and then with Src, and that, upon its palmitoylation, binding to cholestol may occur, a mechanism that may explain the robust detection of PKCε in the rafts in response to R(+)-MA (Fig. 5).

Furthermore, our data demonstrate that activation of PKCε alone suffices to produce a rather prolonged activation of Ras in neurons. Activation of PKCs with the phorbol ester TPA has long been shown to cause Ras (Fig. 3C) and Raf activation (e.g., Zisopoulou et al., 2013), yet the mechanism still remains unknown. Interestingly, activation of Ras with R(+)-MA differed in that it was biphasic (Fig. 3B), a mode that we have previously shown for ERK activation by RMA (Asimaki and Mangoura, 2011). Ras activation after GPCR agonism, most often

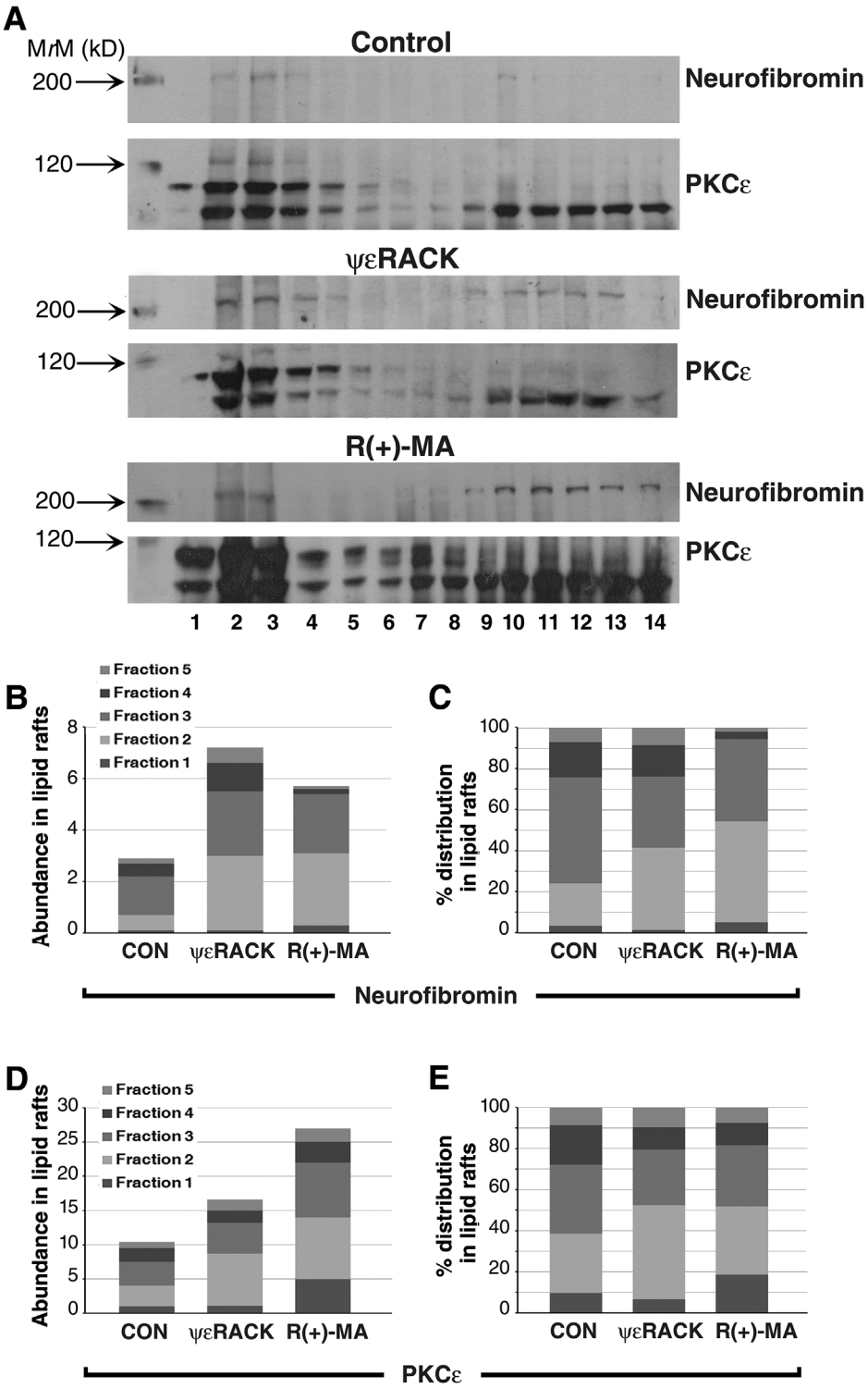

Fig. 5. PKCε activation leads to its enrichment in lipid rafts along with its substrate RasGAP neurofibromin. A. Frames contain representative images from E11 telencephali exposed to vehicle, ψεRACK, or R(+)-MA for 3 min. Each lane contains a 50 μl aliquot from each OptiPrep gradient fraction, analyzed by SDS 7%-polyacrylamide gel electrophoresis and by Western blotting with indicated specific antibodies (2.1); arrows point to pre-stained markers with indicated Mr. **B - E.** Densitometry analysis of the abundance of neurofibromin and PKCε in lipid rafts (fractions 1–5); values in B and D are the mean of neurofibromin and PKCε immunoreactivity from 3 to 5 experiments (SEM was ≤5% in all cases), while values in C and E represent the percentage of immunoreactivity in each of the five lipid fractions.

predicted from activation of Rafs or MAPKs, is known to require a number of effectors, most prominently of PKC, Src-family kinases, and the transactivation of RTKs (Daub et al., 1996; Luttrell et al., 1996), yet the details remain sketchy. Specifically for CB1R, we have postulated that the earliest signalling event is a Gq/11-mediated phospholipase C and PKCε activation; CB1 and PKCε then dissociate due to conformational changes in CB1 and to the PLC/DAG-induced "opening" (activation) of PKCε, with the latter preferentially associating with Src-family kinases (Song et al., 2002) to activate them (Asimaki and Mangoura, 2011). This CB1/Gq/PLC/PKCε/Src–Fyn leads to Raf activation and a first peak of ERK activation (Asimaki and Mangoura, 2011), most likely after the first peak of Ras activation that we now show (Fig. 3). Moreover, we now may attribute the second peak of Ras activation (Fig. 3) in transactivation of FGFR, which we have shown to occur via a second pathway CB1/Gi/PKCε/Src–Fyn and intermolecular Src and FGFR phosphorylations (Asimaki and Mangoura, 2011; Sandilands et al., 2007).

In both cases recruitment of RasGEFs to membranes would be necessary, towards which we now demonstrate that the PKCε and Ras activation temporal profiles correlate well with recruitment of SOS1 to

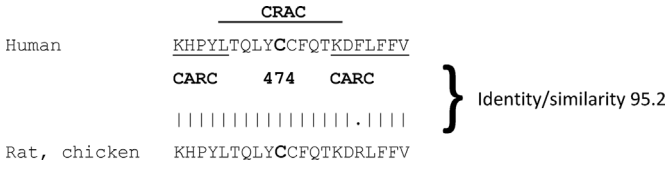

Scheme 1. Predicted cholestol-binding motifs surround the verified site of palmitoylation Cys 474 of PKCε. Amino acid pairwise sequence alignments, which correspond to a 21 residue region, centered around Cys 474 in three animal species, namely, *Homo sapiens*, *Rattus norvegicus*, and *Gallus gallus* revealed high degree of conservation with a 95.2% identity/similarity for this sequential CARC-CRAC-CARC motif ("·" indicate no alignment).

lipid rafts, an almost undetectable event in basal conditions (Fig. 4). The mechanistics of GPCR-mediated activation of RasGEFs remains largely unknown as well (Xu, 2018), while for RTK agonism it is generally accepted that tyrosine phosphorylation of Grb2 will escort SOS1 to membranes, where SOS1 will bind Ras for its full activation as a RasGEF (Christensen et al., 2016). Indeed we observed a transient, low, yet distinct and specific enrichment of SOS1 in the rafts by ψεRACK or methanandamide. However, after CB1R activation, SOS1 was also detected in the Golgi membrane fractions along with P- PKCε (Fig. 2C) PKCε (Fig. 5) and neurofibromin (Fig. 5), suggesting intense and instant endocytosis, whereas this process was lesser with ψεRACK, explaining the longer duration of Ras activation with ψεRACK. Thus, our results are in accordance with recent studies concerned with the removal of SOS1 from the membrane and the termination of the signal, as a single SOS molecule can progressively activate thousands of Ras molecules, which showed that a membrane-recruited SOS continuously activates Ras until it is actively removed via endocytosis (Christensen et al., 2016).

The common principle for both GEFs and GAPs to act upon the farnesylated and palmitoylated Ras is to necessarily translocate to the membrane, a process that affords the known cell-type specific regulation of Ras signalling output. Proximal positioning at a 2D surface has been suggested to afford local concentration increases equal to five orders of magnitude increase in binding constant over free solution or cytosolic concentrations (Simanshu et al., 2017). We now show for the first time that the RasGAP neurofibromin acutely associates with specific plasma membrane domains in a PKCε-regulated manner (Fig. 5). The enrichment of this bona fide PKCε substrate (Mangoura et al., 2006; Leondaritis et al., 2009; Koliou et al., 2016) in the more ordered membrane was over > 3-fold after acute exposure to ψεRACK or R (+)-MA (Fig. 5) and we may assume that this would significantly increase its binding to H-Ras for inactivation.

The profile of neurofibromin distribution among the fractionated membranes we describe here resembles those of prenylated and/or acylated proteins, usually found at the inner leaflet of the plasma membrane or at endomembranes. However, none of the known lipid modifications that lead signalling proteins to lipid rafts has been shown for neurofibromin, a possibility we have now emphasized and further addressed with in silico analysis for lipid modifications. We dismissed a myristoylation site at position 26 of neurofibromin, as there was no caspase substrate motif in the preceding sequence, necessary for proteolytic cleavage and exposure of an internal glycine (Zha et al., 2000). Because several neuronal proteins are targeted to cholesterol-rich membranes posttranslationally by palmitoylation, like the soluble enzyme GAD65 (Kanaani et al., 2002), we next screened neurofibromin for palmitoylation sites. While Cysteine 1365 is unique for the GRD type I (Human transcript 201, GRDI) (Table 1), some of the rest predicted palmitoylation sites should be discussed because they are highly probable, highly conserved (> 96%) between human and *Gallus gallus* (chicken), and clustered in the N-terminus cysteine/serine-rich domain (CSRD, residues 543–909) which is an important allosteric activator the RasGAP activity of the adjacent GRD after PKC-dependent phosphorylation, sufficient to switch the biological effects of EGF signalling (Mangoura et al., 2006). Moreover, recent genetic analysis has pinpointed mutations in CSRD as associated with a higher risk of developing optic pathway glioma (Xu et al., 2018), while in a large cohort of NF-1 patients severe phenotypes were more prevalent with missense mutations affecting only one of five neighboring amino acids, 844–848 (Koczkowska et al., 2018). Within this stretch, Cysteine 845 is a highly probable palmitoylation site and mutations in any of the other four amino acids would also abrogate the motif.

Proximity analysis of the cholesterol binding motifs to putative palmitoylations sites showed that, while neurofibromin contains many CARC (38) and CRAC (22) motifs across its sequence, one is in close proximity with the unique to GRD type I transcript Cys-1365 (Table 1). Therefore, our in silico analysis predicts that both the palmitoylation site Cys-1365 and the cholesterol motif at 1364–1375 will be abrogated in the products of the GRD type II transcripts, thus lending an explanation for the known weaker RasGAP activity of GRD type II neurofibromin (Andersen et al., 1993; Leondaritis and Mangoura, 2010).

Summarizing, our studies postulate that in neurons, CB1-dependent activation of PKCε increases its own affinity for the lipid rafts and that in a coordinated manner of both the RasGEF SOS1 and the RasGAP neurofibromin. These results imply that regulated, transient neurofibromin concentrations may filter out the plethora of SOS1-activated H-Ras molecules available for mobility towards the less ordered membranes, thus controlling downstream signalling output in neurons.

Table 1
Proximity of putative plamitoylation and cholesterol binding sites. Comparative analysis GRDI and GRDII types in human and chicken postulate a. full identity for these amino acid regions, and b. that insertion of exon 32, which results in the translation of the weaker RasGAP GRDII, abrogates a cholesterol binding site in both species, numbers refer to Ensembl annotations.

Palmitoylation site (predicted)	Position (aa)	Transcript	Cholesterol binding sites (predicted)	Position (aa)	Neurofibromin domain
SSQMLFYI**C**KKLTSHQ	582	Both Human 201 (GRDI) and Human 202 (GRDII)			CSRD
KQADRSS**C**HFLLFYG	622				
SMDSAAG**C**SGTPPIC	673				
AVLVAMS**C**FRHLCEE	709				
CEEADIR**C**GVDEVSV	721				
INMTGFL**C**ALGGVCL	845				
RLLSLMV**C**NHEKVGL	904				
PPQLRSV**C**HCLYQVV	1365	Only Human 201 (GRDI)	V**C**HCLYQVVSQR	1364–1375	GRD type I
SQMLFYI**C**KKLTSHQ	597	Both gga NF1-204 (GRDII) and gga NF1-203			CSRD
KQSDRTS**C**HFLFLYD	637	(GRDI)			
SMESTAG**C**SGTPIC**R**	684				
AVLVAMS**C**FRHLCEE	719				
CEEADIR**C**GVDEVSV	731				
INMTGFL**C**ALGGVCL	855				
RLLTLMV**C**NHEKVGL	914				
PPQLRSV**C**HCLYQVV	1360	Only gga NF1-203 (GRDI)	V**C**HCLYQVVSQR	1359–1370	GRD type I

Acknowledgements

The authors would like to thank Dr. George Leondaritis for his help with lipid rafts characterizations and discussions. This work was partially supported by PENED (grant 03ED778) from the Greek Secretariat for Research and Technology (DM, ET, and SK) and Biomedical Research Foundation of the Academy of Athens funds (DM).

References

Alpar, A., Naumann, N., Hartig, W., Arendt, T., Gartner, U., 2008. Enhanced Ras activity preserves dendritic size and extension as well as synaptic contacts of neurons after functional deprivation in synRas mice. Eur. J. Neurosci. 27, 3083–3094.

Andersen, L.B., Ballester, R., Marchuk, D.A., Chang, E., Gutmann, D.H., Saulino, A.M., Camonis, J., Wigler, M., Collins, F.S., 1993. A conserved alternative splice in the von Recklinghausen neurofibromatosis (NF1) gene produces two neurofibromin isoforms, both of which have GTPase-activating protein activity. Mol. Cell. Biol. 13, 487–495.

Aoki, Y., Niihori, T., Kawame, H., Kurosawa, K., Ohashi, H., Tanaka, Y., Filocamo, M., Kato, K., Suzuki, Y., Kure, S., Matsubara, Y., 2005. Germline mutations in HRAS proto-oncogene cause Costello syndrome. Nat. Genet. 37, 1038–1040.

Asimaki, O., Leondaritis, G., Lois, G., Sakellaridis, N., Mangoura, D., 2011. Cannabinoid 1 receptor-dependent transactivation of fibroblast growth factor receptor 1 emanates from lipid rafts and amplifies extracellular signal-regulated kinase 1/2 activation in embryonic cortical neurons. J. Neurochem. 116, 866–873.

Asimaki, O., Mangoura, D., 2011. Cannabinoid receptor 1 induces a biphasic ERK activation via multiprotein signaling complex formation of proximal kinases PKCepsilon, Src, and Fyn in primary neurons. Neurochem. Int. 58, 135–144.

Baizer, L., Ciment, G., Hendrickson, S.K., Schafer, G.L., 1993. Regulated expression of the neurofibromin type I transcript in the developing chicken brain. J. Neurochem. 61, 2054–2060.

Barron, V.A., Lou, H., 2012. Alternative splicing of the neurofibromatosis type I pre-mRNA. Biosci. Rep. 32, 131–138.

Bluthgen, N., van Bentum, M., Merz, B., Kuhl, D., Hermey, G., 2017. Profiling the MAPK/ERK dependent and independent activity regulated transcriptional programs in the murine hippocampus in vivo. Sci. Rep. 7, 45101.

Bollag, G., Clapp, D.W., Shih, S., Adler, F., Zhang, Y.Y., Thompson, P., Lange, B.J., Freedman, M.H., McCormick, F., Jacks, T., Shannon, K., 1996. Loss of NF1 results in activation of the Ras signaling pathway and leads to aberrant growth in haematopoietic cells. Nat. Genet. 12, 144–148.

Brandman, R., Disatnik, M.H., Churchill, E., Mochly-Rosen, D., 2007. Peptides derived from the C2 domain of protein kinase C epsilon (epsilon PKC) modulate epsilon PKC activity and identify potential protein-protein interaction surfaces. J. Biol. Chem. 282, 4113–4123.

Brannan, C.I., Perkins, A.S., Vogel, K.S., Ratner, N., Nordlund, M.L., Reid, S.W., Buchberg, A.M., Jenkins, N.A., Parada, L.F., Copeland, N.G., 1994. Targeted disruption of the neurofibromatosis type-1 gene leads to developmental abnormalities in heart and various neural crest-derived tissues. Genes Dev. 8, 1019–1029.

Brems, H., Beert, E., de Ravel, T., Legius, E., 2009. Mechanisms in the pathogenesis of malignant tumours in neurofibromatosis type 1. Lancet Oncol. 10, 508–515.

Brown, J.A., Emnett, R.J., White, C.R., Yuede, C.M., Conyers, S.B., O'Malley, K.L., Wozniak, D.F., Gutmann, D.H., 2010. Reduced striatal dopamine underlies the attention system dysfunction in neurofibromatosis-1 mutant mice. Hum. Mol. Genet. 19, 4515–4528.

Cabrera-Poch, N., Sanchez-Ruiloba, L., Rodriguez-Martinez, M., Iglesias, T., 2004. Lipid raft disruption triggers protein kinase C and Src-dependent protein kinase D activation and Kidins220 phosphorylation in neuronal cells. J. Biol. Chem. 279, 28592–28602.

Calabrese, B., Halpain, S., 2005. Essential role for the PKC target MARCKS in maintaining dendritic spine morphology. Neuron 48, 77–90.

Cheng, Y., Leung, S., Mangoura, D., 2000. Transient suppression of cortactin ectopically induces large telencephalic neurons towards a GABAergic phenotype. J. Cell Sci. 113 (Pt 18), 3161–3172.

Cherezov, V., Rosenbaum, D.M., Hanson, M.A., Rasmussen, S.G., Thian, F.S., Kobilka, T.S., Choi, H.J., Kuhn, P., Weis, W.I., Kobilka, B.K., Stevens, R.C., 2007. High-resolution crystal structure of an engineered human beta2-adrenergic G protein-coupled receptor. Science 318, 1258–1265.

Christensen, S.M., Tu, H.L., Jun, J.E., Alvarez, S., Triplet, M.G., Iwig, J.S., Yadav, K.K., Bar-Sagi, D., Roose, J.P., Groves, J.T., 2016. One-way membrane trafficking of SOS in receptor-triggered Ras activation. Nat. Struct. Mol. Biol. 23, 838–846.

Dasgupta, S., Bhattacharya, S., Maitra, S., Pal, D., Majumdar, S.S., Datta, A., Bhattacharya, S., 2011. Mechanism of lipid induced insulin resistance: activated PKCepsilon is a key regulator. Biochim. Biophys. Acta 1812, 495–506.

Daub, H., Weiss, F.U., Wallasch, C., Ullrich, A., 1996. Role of transactivation of the EGF receptor in signalling by G-protein-coupled receptors. Nature 379, 557–560.

de Rooij, J., Bos, J.L., 1997. Minimal Ras-binding domain of Raf1 can be used as an activation-specific probe for Ras. Oncogene 14, 623–625.

Ebinu, J.O., Bottorff, D.A., Chan, E.Y., Stang, S.L., Dunn, R.J., Stone, J.C., 1998. RasGRP, a Ras guanyl nucleotide- releasing protein with calcium- and diacylglycerol-binding motifs. Science 280, 1082–1086.

Fantini, J., Barrantes, F.J., 2013. How cholesterol interacts with membrane proteins: an exploration of cholesterol-binding sites including CRAC, CARC, and tilted domains. Front. Physiol. 4, 31.

Fedonidis, C., Alexakis, N., Koliou, X., Asimaki, O., Tsirimonaki, E., Mangoura, D., 2014. Long-term changes in the ghrelin-CB1R axis associated with the maintenance of lower body weight after sleeve gastrectomy. Nutr. Diabetes 4, e127.

Gauthier-Kemper, A., Igaev, M., Sundermann, F., Janning, D., Bruhmann, J., Moschner, K., Reyher, H.J., Junge, W., Glebov, K., Walter, J., Bakota, L., Brandt, R., 2014. Interplay between phosphorylation and palmitoylation mediates plasma membrane targeting and sorting of GAP43. Mol. Biol. Cell 25, 3284–3299.

Grewal, T., Koese, M., Tebar, F., Enrich, C., 2011. Differential regulation of RasGAPs in cancer. Genes Cancer 2, 288–297.

Hyman, S.L., Shores, A., North, K.N., 2005. The nature and frequency of cognitive deficits in children with neurofibromatosis type 1. Neurology 65, 1037–1044.

Kanaani, J., el-Husseini Ael, D., Aguilera-Moreno, A., Diacovo, J.M., Bredt, D.S., Baekkeskov, S., 2002. A combination of three distinct trafficking signals mediates axonal targeting and presynaptic clustering of GAD65. J. Cell Biol. 158, 1229–1238.

Kawakami, Y., Kitaura, J., Yao, L., McHenry, R.W., Kawakami, Y., Newton, A.C., Kang, S., Kato, R.M., Leitges, M., Rawlings, D.J., Kawakami, T., 2003. A Ras activation pathway dependent on Syk phosphorylation of protein kinase C. Proc. Natl. Acad. Sci. U. S. A. 100, 9470–9475.

Kim, S.E., Yoon, J.Y., Jeong, W.J., Jeon, S.H., Park, Y., Yoon, J.B., Park, Y.N., Kim, H., Choi, K.Y., 2009. H-Ras is degraded by Wnt/β-catenin signaling via β-TrCP-mediated polyubiquitylation. J. Cell Sci., vol. 122, 842–848.

Koczkowska, M., Chen, Y., Callens, T., Gomes, A., Sharp, A., Johnson, S., Hsiao, M.C., Chen, Z., Balasubramanian, M., Barnett, C.P., Becker, T.A., Ben-Shachar, S., Bertola, D.R., Blakeley, J.O., Burkitt-Wright, E.M.M., Callaway, A., Crenshaw, M., Cunha, K.S., Cunningham, M., D'Agostino, M.D., Dahan, K., De Luca, A., Destree, A., Dhamija, R., Eoli, M., Evans, D.G.R., Galvin-Parton, P., George-Abraham, J.K., Gripp, K.W., Guevara-Campos, J., Hanchard, N.A., Hernandez-Chico, C., Immken, L., Janssens, S., Jones, K.J., Keena, B.A., Kochhar, A., Liebelt, J., Martir-Negron, A., Mahoney, M.J., Maystadt, I., McDougall, C., McEntagart, M., Mendelsohn, N., Miller, D.T., Mortier, G., Morton, J., Pappas, J., Plotkin, S.R., Pond, D., Rosenbaum, K., Rubin, K., Russell, L., Rutledge, L.S., Saletti, V., Schonberg, R., Schreiber, A., Seidel, M., Siqveland, E., Stockton, D.W., Trevisson, E., Ullrich, N.J., Upadhyaya, M., van Minkelen, R., Verhelst, H., Wallace, M.R., Yap, Y.S., Zackai, E., Zonana, J., Zurcher, V., Claes, K., Martin, Y., Korf, B.R., Legius, E., Messiaen, L.M., 2018. Genotype-Phenotype correlation in NF1: evidence for a more severe phenotype Associated with missense mutations affecting NF1 codons 844-848. Am. J. Hum. Genet. 102, 69–87.

Koliou, X., Fedonidis, C., Kalpachidou, T., Mangoura, D., 2016. Nuclear import mechanism of neurofibromin for localization on the spindle and function in chromosome congression. J. Neurochem. 136, 78–91.

Lang, M.L., Chen, Y.W., Shen, L., Gao, H., Lang, G.A., Wade, T.K., Wade, W.F., 2002. IgA Fc receptor (FcalphaR) cross-linking recruits tyrosine kinases, phosphoinositide kinases and serine/threonine kinases to glycolipid rafts. Biochem. J. 364, 517–525.

Leondaritis, G., Petrikkos, L., Mangoura, D., 2009. Regulation of the Ras-GTPase activating protein neurofibromin by C-tail phosphorylation: implications for protein kinase C/Ras/extracellular signal-regulated kinase 1/2 pathway signaling and neuronal differentiation. J. Neurochem. 109, 573–583.

Leondaritis, G., Mangoura, D., 2010. Regulation of neurofibromin's GAP-related domain RasGAP activity by a Sec14-homology domain-dependent allosteric switch. Trans. 61th EEBMB. A17, 57.

Levental, I., Grzybek, M., Simons, K., 2010. Greasing their way: lipid modifications determine protein association with membrane rafts. Biochemistry 49, 6305–6316.

Li, C., Cheng, Y., Gutmann, D.A., Mangoura, D., 2001. Differential localization of the neurofibromatosis 1 (NF1) gene product, neurofibromin, with the F-actin or microtubule cytoskeleton during differentiation of telencephalic neurons. Brain Res Dev Brain Res 130, 231–248.

Lin, Y.L., Lei, Y.T., Hong, C.J., Hsueh, Y.P., 2007. Syndecan-2 induces filopodia and dendritic spine formation via the neurofibromin-PKA-Ena/VASP pathway. J. Cell Biol. 177, 829–841.

Luo, G., Kim, J., Song, K., 2014. The C-terminal domains of human neurofibromin and its budding yeast homologs Ira1 and Ira2 regulate the metaphase to anaphase transition. Cell Cycle 13, 2780–2789.

Luttrell, L.M., Hawes, B.E., van Biesen, T., Luttrell, D.K., Lansing, T.J., Lefkowitz, R.J., 1996. Role of c-Src tyrosine kinase in G protein-coupled receptor- and Gbetagamma subunit-mediated activation of mitogen-activated protein kinases. J. Biol. Chem. 271, 19443–19450.

Macdonald, J.L., Pike, L.J., 2005. A simplified method for the preparation of detergent-free lipid rafts. J. Lipid Res. 46, 1061–1067.

Mangoura, D., Asimaki, O., Tsirimonaki, E., Sakellaridis, N., 2016. Role of lipid rafts and the underlying filamentous-actin cytoskeleton in cannabinoid receptor 1 signaling. In: Preedy, V. (Ed.), Neuropathology of Drug Addictions and Substance Misuse. Academic Press, pp. 689–701.

Mangoura, D., Dawson, G., 1993. Opioid peptides activate phospholipase D and protein kinase C-epsilon in chicken embryo neuron cultures. Proc. Natl. Acad. Sci. U. S. A. 90, 2915–2919.

Mangoura, D., Dawson, G., 1998. Programmed cell death in cortical chick embryo astrocytes is associated with activation of protein kinase PK60 and ceramide formation. J. Neurochem. 70, 130–138.

Mangoura, D., Sogos, V., Dawson, G., 1993. Protein kinase C-epsilon is a developmentally regulated, neuronal isoform in the chick embryo central nervous system. J. Neurosci. Res. 35, 488–498.

Mangoura, D., Sun, Y., Li, C., Singh, D., Gutmann, D.H., Flores, A., Ahmed, M., Vallianatos, G., 2006. Phosphorylation of neurofibromin by PKC is a possible molecular switch in EGF receptor signaling in neural cells. Oncogene 25, 735–745.

Marais, R., Light, Y., Mason, C., Paterson, H., Olson, M.F., Marshall, C.J., 1998. Requirement of Ras-GTP-Raf complexes for activation of Raf-1 by protein kinase C. Science 280, 109–112.

Mellert, K., Lechner, S., Ludeke, M., Lamla, M., Moller, P., Kemkemer, R., Scheffzek, K.,

Kaufmann, D., 2018. Restoring functional neurofibromin by protein transduction. Sci. Rep. 8, 6171.
Nishi, T., Lee, P.S., Oka, K., Levin, V.A., Tanase, S., Morino, Y., Saya, H., 1991. Differential expression of two types of the neurofibromatosis type 1 (NF1) gene transcripts related to neuronal differentiation. Oncogene 6, 1555–1559.
O'Hayre, M., Eichel, K., Avino, S., Zhao, X., Steffen, D.J., Feng, X., Kawakami, K., Aoki, J., Messer, K., Sunahara, R., Inoue, A., von Zastrow, M., Gutkind, J.S., 2017. Genetic evidence that beta-arrestins are dispensable for the initiation of beta2-adrenergic receptor signaling to ERK. Sci. Signal. 10.
Oddi, S., Dainese, E., Sandiford, S., Fezza, F., Lanuti, M., Chiurchiu, V., Totaro, A., Catanzaro, G., Barcaroli, D., De Laurenzi, V., Centonze, D., Mukhopadhyay, S., Selent, J., Howlett, A.C., Maccarrone, M., 2012. Effects of palmitoylation of Cys(415) in helix 8 of the CB(1) cannabinoid receptor on membrane localization and signalling. Br. J. Pharmacol. 165, 2635–2651.
Oliveira, A.F., Yasuda, R., 2014. Neurofibromin is the major ras inactivator in dendritic spines. J. Neurosci. 34, 776–783.
Ong, S.H., Guy, G.R., Hadari, Y.R., Laks, S., Gotoh, N., Schlessinger, J., Lax, I., 2000. FRS2 proteins recruit intracellular signaling pathways by binding to diverse targets on fibroblast growth factor and nerve growth factor receptors. Mol. Cell. Biol. 20, 979–989.
Pechlivanis, M., Kuhlmann, J., 2006. Hydrophobic modifications of Ras proteins by isoprenoid groups and fatty acids–More than just membrane anchoring. Biochim. Biophys. Acta 1764, 1914–1931.
Prior, I.A., Harding, A., Yan, J., Sluimer, J., Parton, R.G., Hancock, J.F., 2001. GTP-dependent segregation of H-ras from lipid rafts is required for biological activity. Nat. Cell Biol. 3, 368–375.
Raman, M., Chen, W., Cobb, M.H., 2007. Differential regulation and properties of MAPKs. Oncogene 26, 3100–3112.
Salaun, C., Gould, G.W., Chamberlain, L.H., 2005. The SNARE proteins SNAP-25 and SNAP-23 display different affinities for lipid rafts in PC12 cells. Regulation by distinct cysteine-rich domains. J. Biol. Chem. 280, 1236–1240.
Samuels, I.S., Karlo, J.C., Faruzzi, A.N., Pickering, K., Herrup, K., Sweatt, J.D., Saitta, S.C., Landreth, G.E., 2008. Deletion of ERK2 mitogen-activated protein kinase identifies its key roles in cortical neurogenesis and cognitive function. J. Neurosci. 28, 6983–6995.
Sanders, S.S., Martin, D.D., Butland, S.L., Lavallee-Adam, M., Calzolari, D., Kay, C., Yates 3rd, J.R., Hayden, M.R., 2015. Curation of the mammalian palmitoylome indicates a pivotal role for palmitoylation in diseases and disorders of the nervous system and cancers. PLoS Comput. Biol. 11, e1004405.
Sandilands, E., Akbarzadeh, S., Vecchione, A., McEwan, D.G., Frame, M.C., Heath, J.K., 2007. Src kinase modulates the activation, transport and signalling dynamics of fibroblast growth factor receptors. EMBO Rep. 8, 1162–1169.
Seeger, G., Gartner, U., Holzer, M., Arendt, T., 2003. Constitutive expression of p21H-Ras (Val12) in neurons induces increased axonal size and dendritic microtubule density in vivo. J. Neurosci. Res. 74, 868–874.
Sen, A., Hongpaisan, J., Wang, D., Nelson, T.J., Alkon, D.L., 2016. Protein kinase C (PKC) promotes synaptogenesis through membrane accumulation of the postsynaptic density protein PSD-95. J. Biol. Chem. 291, 16462–16476.
Scheffzek, K., Shivalingaiah, G., 2019. Ras-specific GTPase-activating proteins—-structures, mechanisms, and interactions. Cold Spring Harb Perspect Med 9 (3) pii.a031500.
Simanshu, D.K., Nissley, D.V., McCormick, F., 2017. RAS proteins and their regulators in human Disease. Cell 170, 17–33.
Smotrys, J.E., Linder, M.E., 2004. Palmitoylation of intracellular signaling proteins: regulation and function. Annu. Rev. Biochem. 73, 559–587.
Song, C., Vondriska, T.M., Wang, G.W., Klein, J.B., Cao, X., Zhang, J., Kang, Y.J., D'Souza, S., Ping, P., 2002. Molecular conformation dictates signaling module formation: example of PKCepsilon and Src tyrosine kinase. Am. J. Physiol. Heart Circ. Physiol. 282, H1166–H1171.
Starinsky-Elbaz, S., Faigenbloom, L., Friedman, E., Stein, R., Kloog, Y., 2009. The pre-GAP-related domain of neurofibromin regulates cell migration through the LIM kinase/cofilin pathway. Mol. Cell. Neurosci. 42, 278–287.
Tartaglia, M., Mehler, E.L., Goldberg, R., Zampino, G., Brunner, H.G., Kremer, H., van der Burgt, I., Crosby, A.H., Ion, A., Jeffery, S., Kalidas, K., Patton, M.A., Kucherlapati, R.S., Gelb, B.D., 2001. Mutations in PTPN11, encoding the protein tyrosine phosphatase SHP-2, cause Noonan syndrome. Nat. Genet. 29, 465–468.
Thelen, M., Rosen, A., Nairn, A.C., Aderem, A., 1991. Regulation by phosphorylation of reversible association of a myristoylated protein kinase C substrate with the plasma membrane. Nature 351, 320–322.
Xu, M., Xiong, H., Han, Y., Li, C., Mai, S., Huang, Z., Ai, X., Guo, Z., Zeng, F., Guo, Q., 2018. Identification of mutation regions on NF1 responsible for high- and low-risk development of optic pathway glioma in neurofibromatosis type I. Front. Genet. 9, 270.
Tsirimonaki, E., Fedonidis, C., Pneumaticos, S., Tragas, A., Michalopoulos, I., Mangoura, D., et al., 2013. PKCε signalling activates ERK1/2, and regulates Aggrecan, ADAMTS5, and miR377 gene expression in human nucleus pulposus cells. PLoS One 8 (11), e82045.
Xu, X., 2018. Filling GAPs in G protein- coupled receptor (GPCR)-mediated Ras adaptation and chemotaxis. Small GTPases 1–3.
Yamaguchi, H., Shiraishi, M., Fukami, K., Tanabe, A., Ikeda-Matsuo, Y., Naito, Y., Sasaki, Y., 2009. MARCKS regulates lamellipodia formation induced by IGF-I via association with PIP2 and beta-actin at membrane microdomains. J. Cell. Physiol. 220, 748–755.
Zha, J., Weiler, S., Oh, K.J., Wei, M.C., Korsmeyer, S.J., 2000. Posttranslational N-myristoylation of BID as a molecular switch for targeting mitochondria and apoptosis. Science 290, 1761–1765.
Zhang, G., Kazanietz, M.G., Blumberg, P.M., Hurley, J.H., 1995. Crystal structure of the cys2 activator-binding domain of protein kinase C delta in complex with phorbol ester. Cell 81, 917–924.
Zhu, Y., Romero, M.I., Ghosh, P., Ye, Z., Charnay, P., Rushing, E.J., Marth, J.D., Parada, L.F., 2001. Ablation of NF1 function in neurons induces abnormal development of cerebral cortex and reactive gliosis in the brain. Genes Dev. 15, 859–876.
Zisopoulou, S., Asimaki, O., Leondaritis, G., Vasilaki, A., Sakellaridis, N., Pitsikas, N., Mangoura, D., 2013. PKC-epsilon activation is required for recognition memory in the rat. Behav. Brain Res. 253, 280–289.